Journal of *Marine Science and Engineering*

MDPI

Article

Stress Response in Toxic Diatoms: The Effects of Abiotic Factors on Growth and RNA Content in *Pseudo-nitzschia calliantha* and in *Pseudo-nitzschia multistriata*

Luca Ambrosino [1,†], Marco Miralto [1,†], Lucia Barra [2,†], Angela Sardo [3,*], Maria Luisa Chiusano [1,4], Radiana Cozza [5], Michele Ferrari [5] and Silvestro Greco [6]

[1] Research Infrastructures for Marine Biological Resources Department (RIMAR), Stazione Zoologica Anton Dohrn, Villa Comunale, 80121 Naples, Italy; luca.ambrosino@szn.it (L.A.); marco.miralto@szn.it (M.M.); chiusano@unina.it (M.L.C.)
[2] Department of Ecosustainable Marine Biotechnology (BLUBIO), Stazione Zoologica Anton Dohrn, Calabria Marine Centre, Contrada Torre Spaccata, 87071 Amendolara, Italy; lucia.barra@szn.it
[3] Department of Ecosustainable Marine Biotechnology (BLUBIO), Stazione Zoologica Anton Dohrn, Via Ammiraglio Ferdinando Acton 55, 80133 Naples, Italy
[4] Department of Agricultural Sciences, University of Naples Federico II, Portici, 80055 Naples, Italy
[5] Department of Biology, Ecology and Earth Science, University of Calabria, Arcavacata di Rende, 87036 Cosenza, Italy; radiana.cozza@unical.it (R.C.); michele.ferrari@unical.it (M.F.)
[6] Department of Integrative Marine Ecology (EMI) Stazione Zoologica Anton Dohrn, Calabria Marine Centre, Contrada Torre Spaccata, 87071 Amendolara, Italy; silvestro.greco@szn.it
* Correspondence: angela.sardo@szn.it
† These authors contributed equally to this work.

Abstract: Pennate diatoms belonging to the genus *Pseudo-nitzschia* are important components of phytoplankton assemblages in aquatic environments. Among them, the bloom-forming species *Pseudo-nitzschia calliantha* and *Pseudo-nitzschia multistriata* are known as domoic acid producers, and are thus considered harmful for aquatic organisms and for human health. For these reasons, monitoring the abundance of such species, as well as identifying the growth conditions enhancing or inhibiting their growth, could help to predict eventual risks for aquatic communities and for humans by direct or indirect exposure to these toxic algae. In this work, we assessed the effects of different parameters (irradiance, temperature, salinity, and nutrients) on six *Pseudo-nitzschia* species by evaluating their specific growth rates and total RNA content. Our results—corroborated by statistical analyses of regression and correlation plots of control samples and samples exposed to stressful conditions, showed, as expected, a general decrease in growth rates under suboptimal levels of temperature, irradiance, salinity, and nutrient supply (especially under silicon depletion), that was usually accomplished by a general increase in RNA content inside cells. We hypothesized that increments in RNA levels in cells exposed to unfavorable conditions could be due to a relatively fast activation of the mechanisms of stress response.

Keywords: *Pseudo-nitzschia* spp.; thermal stress; irradiance stress; salinity stress; nutrient depletion; statistical analysis; algal growth; RNA content variation

check for updates

Citation: Ambrosino, L.; Miralto, M.; Barra, L.; Sardo, A.; Chiusano, M.L.; Cozza, R.; Ferrari, M.; Greco, S. Stress Response in Toxic Diatoms: The Effects of Abiotic Factors on Growth and RNA Content in *Pseudo-nitzschia calliantha* and in *Pseudo-nitzschia multistriata*. *J. Mar. Sci. Eng.* **2023**, *11*, 1743. https://doi.org/10.3390/jmse11091743

Received: 5 August 2023
Revised: 31 August 2023
Accepted: 2 September 2023
Published: 5 September 2023

Copyright: © 2023 by the authors. Licensee MDPI, Basel, Switzerland. This article is an open access article distributed under the terms and conditions of the Creative Commons Attribution (CC BY) license (https://creativecommons.org/licenses/by/4.0/).

1. Introduction

Planktonic algae, responsible for most of the net primary production (NPP), are the main food source for filter-feeding organisms as well as for larvae of commercially important crustaceans and finfish [1]. In some cases, the proliferation of planktonic non-toxic algae can be beneficial to extensive aquaculture ponds and wild fishery operations [2]. However, harmful algal blooms (HABs), e.g., natural blooms of toxic microalgae (mostly belonging to dinoflagellates and diatoms classes), can cause severe economic losses to aquaculture, fisheries, and tourism operations, and have detrimental impacts on both

environment and human health [3]. Harmful effects on humans can be caused by direct exposure to toxic algae that cause respiratory distress due to inhalation of aerosols from sea water that contains toxic species and skin irritations due to allergy-like reactions, or by consumption of seafood that has accumulated toxins in HAB-polluted environments. High biomass production and toxic events can be associated with fish mortality due to low oxygen levels, direct toxicity, hemolysis, and mechanical damage [4]. Here, we focused on diatoms, a class of photoautotrophic microalgae present in virtually every aquatic habitat, since they can be found suspended in water columns of rivers, lakes, estuaries, and oceans. Diatoms can produce a range of harmful biotoxins, such as the domoic acid (DA), responsible for amnesic shellfish poisoning (ASP), whose effects in humans include abdominal cramps, diarrhea, headache up to permanent short-term memory loss, coma, and death [5]. Domoic acid is usually produced by species belonging to the *Pseudo-nitzschia* genus. Among the 30 known morpho-species of the *Pseudo-nitzschia* genus, eleven to twelve are known to be potentially toxic [6,7]. In recent decades, global warming and climate change, in terms of temperature, precipitation, and wind, have dramatically compromised the equilibrium of aquatic ecosystems and caused water acidification and significant alterations in biodiversity [8]. Environmental changes have also caused variations in the structure and composition of phytoplankton communities, including an increased frequency of HABs [9]. Nutrient availability, together with light and temperature, are primary determinants of phytoplankton growth and biomass accumulation. There is evidence that the reported increase in HAB events and the increased magnitude of these events is linked to nutrient availability [10,11], and these events are often linked (directly or indirectly) to anthropogenic eutrophication [12]. Several methods of toxic microalgae detection have been developed in the last few years, including the use of the microarrays. Microarrays are basically glass microscope slides coated with specific nucleotide-sequence probes, which are used to hybridize with similar target sequences. In the last decade, the use of RNA probes has been considered a useful tool for a fast detection of toxic bloom-forming species [13]. Conventional methods such as identification using light microscopy (LM) and enumeration of cell concentration are time-consuming and not suitable for quickly and specifically identifying marine areas that are potentially dangerous for human health, which could be compromised by direct exposure to these species or through the ingestion of toxin-contaminated seafood. Moreover, identification with an LM is not accurate, since it does not allow us to distinguish between toxic and similar non-toxic strains [14]. For these reasons, the use of RNA probes was approved in the EU Seventh Framework Programme (FP7), and regulated in the "microarrays for the detection of toxic algae" (MIDTAL) project [13,15,16], which employs microarrays designed with SSU and LSU rRNA specific probes for species molecular identification [17]. RNA-based microarrays had been successfully applied for the identification of *Pseudo-nitzschia* species in the natural environment, as well as for the detection of cryptic species. They have also been tested for monitoring species belonging to the genera *Alexandrium*, *Dinophysis*, *Pseudochattonella*, and *Karenia* [13,18–20]. This work aimed to identify the abiotic factors affecting the growth and RNA content of toxic species of *Pseudo-nitzschia*: *P. calliantha* and *P. multistriata*. For this purpose, we exposed these species to different environmental stresses (high and low irradiance, high and low temperature, high and low salinity, and nutrient depletion), and assessed the impact of these factors on cells growth. Moreover, to depict the main aspects associated with the molecular changes of the toxic strains growing under abiotic stresses, we evaluated possible changes in total RNA content. In addition, we considered that studying the ability of the test species to grow under different abiotic stresses and the associated variability in RNA content could be a starting point for calibration of useful signals for possible RNA-based biosensors.

2. Materials and Methods

2.1. Cultivation of Pseudo-nitzschia Strains

Three potentially toxic strains of *P. multistriata* and of *P. calliantha* isolated in the Gulf of Naples in the Spring of 2009 were cultured in f/2 medium [21]. Cultures were maintained

in control conditions: an irradiance of 100 µmol of photons $m^{-2}s^{-1}$ with a 12:12 light:dark cycle, a temperature of 20 °C, and a salinity of 36 PSU. The strains of *P. multistriata* and *P. calliantha* were named Pm1; Pm2; and Pm3, and Pc1; Pc2; and Pc3, respectively.

2.2. Experimental Design

Cells (initial density: 5000 cells/mL, 2000 cells/mL for experiments on salt stress) were cultivated in sterile flasks (total capacity: 50 mL, working volume: 30 mL). To evaluate the effect of temperature, irradiance, or salinity stress, some samples remained in the control conditions, as described above, while others were exposed to higher or lower values of these parameters. For experiments on nutrient depletion, all clones were grown in a modified f/2 medium, in which the molar concentration of the nitrogen source was 580 µM instead of 882 µM, to avoid consistent residuals of this element in the culture medium. However, to obtain a true nutrient starvation, cells were harvested (2000× *g*, 10 min) at the late exponential phase, and then resuspended in a culture medium deprived of one of the three macronutrient sources, namely $NaNO_3$, $NaH_2PO_4 \cdot H_2O$, or $NaSiO_3 \cdot 9H_2O$. According to Dittami and Edvardsen [19], three strains of each species were studied, with parallel experiments being carried out for each strain. The mean values and standard deviations of these three strains are given in the figures and tables. A summary of the experimental design, showing the values of the parameters used in both control and stressful conditions is represented in Table 1. For RNA extraction and quantification, 10 mL subsamples were collected after 24 (Time 1), 48 (Time 2), and 72 (Time 3) hours.

Table 1. Experimental design. Stressful conditions applied to *P. multistriata* strains. (*) $NaNO_3$ molar concentration used in experiments 4–6 before applying nutrient stress was 580 µM.

			Stress Conditions		
Experiment Number	**Control Conditions**	**Abiotic Stress**	**Low**	**High**	**Culture Stage to Apply Stress**
1	20 °C	Temperature	12 °C	28 °C	Exponential
2	100 µmol photons $m^{-2}s^{-1}$	Light	45 µmol photons $m^{-2}s^{-1}$	350 µmol photons $m^{-2}s^{-1}$	Exponential
3	36 PSU	Salinity	34 PSU	38 PSU	Exponential
4	f/2 modified medium *	Nitrogen depletion	0 µM	-	Late exponential
5	f/2 modified medium *	Phosphorous depletion	0 µM	-	Late exponential
6	f/2 modified medium *	Silicon depletion	0 µM	-	Late exponential

2.3. Cell Counts

Cell concentration was evaluated daily in terms of cells/mL and fluorescence values, and estimated through Sedgwick-Rafter chamber counts and Turner fluorometer, respectively. For cell counts, 1 mL samples of both *P. calliantha* and *P. multistriata* clones were preserved in a Lugol's iodine solution (0.1%) and then counted in the Sedgewick-Rafter chamber under light microscopy. Specific growth rate (µ) was calculated for each condition by the following equation:

$$\mu = (\mathrm{Ln}\, C_f - \mathrm{Ln}\, C_0)/(t_f - t_0)$$

where µ is the specific growth rate in exponential phase, C_f is the cell density at the end of exponential phase (t_f), and C_0 represents the algal concentration at the beginning of the exponential phase (t_0).

Algal growth was also evaluated by quantifying light fluoresced by algal samples (4 mL) of all strains with a fluorometer (NB360 Excitation Filter SC415 Emission Filter, Turner, model 110, Dubuque, USA). This was done to verify that cell density and the values

of arbitrary units provided by this instrument showed the same trend. Light intensity was evaluated at 650 nm, which represents the value that gave the maximum absorbance at all growth stages after scanning the wavelength from 550 to 800 nm.

2.4. RNA Extraction

RNA content was evaluated after 72 h in all experimental conditions, following the procedure of Dittami and Edvardsen [19]. This time range was considered useful for detecting short term variation of this parameter, since the final concentration of algal cultures was rarely below 50,000 cells/mL, with the exception of those exposed to high abiotic stresses (see Results). Total RNA extraction was performed by using the TRI-reagent extraction protocol described by Barra and co-workers [18]. The RNA was re-suspended in 20 or 50 µL nuclease-free water and its concentration was measured by Nanodrop 1000 (Agilent Biotechnologies, Singapore).

2.5. Statistical Analysis

Data analysis was performed with in-house-developed tools, using Python3 [22], NumPy [23], and Pandas [24]. In addition, Seaborn [25] was used for data plotting. Observations were first processed to shape a tidy dataset. Direct and inverse linear correlation between variables was studied for both Pm and Pc using Pearson linear coefficient, considering values observed in control and low-, and high-stress conditions for salinity, temperature, and irradiance experiments. Specifically, control versus low-, control versus high-, and high- versus low-stress correlations were studied. Regarding depletion conditions, correlation between control and each of the depletion conditions was studied, together with correlation of the depletion conditions with each other. Raw-observation time series were visualized using a line plot while correlation data were plotted for each experiment using correlation plots. Two-way ANOVA tests without replication related to cell-concentration experiments (cells/mL) were performed. Finally, a heatmap summarizing all the responses in terms of cell growth of both species to the considered stress conditions, was obtained via *heatmapper* web application [26], using as input the Log10 of all the collected cells/mL values.

3. Results

3.1. Irradiance

Light stress was evaluated on *P. multistriata* and *P. calliantha* by inducing an irradiance of 45 and 350 µmol photons m^2 s^{-1} for the low and high treatments, respectively, compared to 100 µE m^{-2} s^{-1} of the control condition. Despite an increase in cell count at 48 h when considering a low-irradiance stress, the effect of irradiance stress on cell growth was distinguishable at 72 h (Figure 1A) in *P. calliantha*, with a general decrease in the number of cells of stressed strains (both high and low irradiance) compared to control conditions. The effect of irradiance on cell growth was more pronounced in *P. multistriata*, since we observed a decrease in the number of cells of both stress conditions (low and high) starting from 48 h (Figure 1B). The correlation plots showed a very strong (0.95) and a strong correlation (0.84) between control and low-irradiance conditions evaluated in terms of cell growth in *P. calliantha* and *P. multistriata*, respectively (Figure 1C,D), highlighting a similar trend in the corresponding time plots (Figure 1A,B). Two-way ANOVA tests performed on both cell-concentration experiments showed significant differences when considering condition*time datasets (p-value of 0.008 and 0.03 for *P. calliantha* and *P. multistriata*, respectively), and non-significant differences when considering condition datasets (Supplementary Tables S1 and S2).

By observing the specific growth rates of both species, we observed a slight decrease in low and high irradiance-stress conditions compared to the control condition (Table 2).

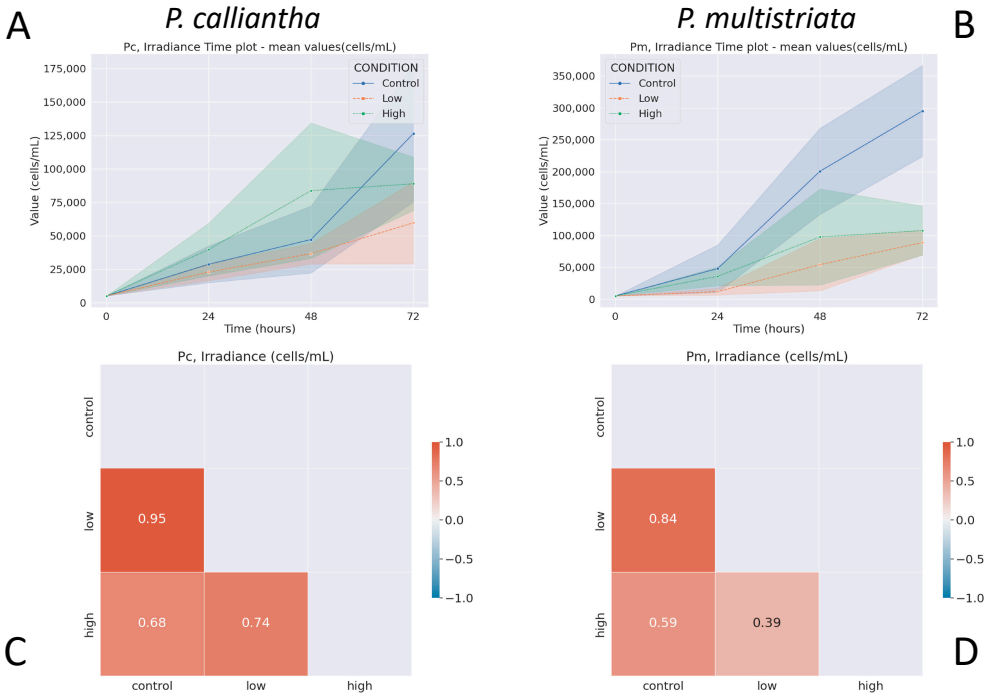

Figure 1. Time plots and correlation plots of cells/mL mean values in response to irradiance in *P. calliantha* (**A**,**C**) and *P. multistriata* (**B**,**D**). An irradiance of 100, 45, and 350 µmol photons $m^{-2}s^{-1}$ was applied for the control, low, and high treatments, respectively. Standard deviations in time plots are shown as color bands, and can partially overlap.

Table 2. Specific growth rate (µ) values related to all the experimental conditions for both *P. calliantha* and *P. multistriata* species. Standard deviations for each µ are also shown.

µ		*P. calliantha*	*P. multistriata*
Irradiance	Control	1.06 ± 0.15	1.35 ± 0.08
	Low	0.80 ± 0.18	0.95 ± 0.08
	High	0.95 ± 0.08	1.01 ± 0.13
Temperature	Control	1.02 ± 0.10	1.11 ± 0.13
	Low	0.79 ± 0.14	0.85 ± 0.15
	High	1.00 ± 0.03	1.11 ± 0.12
Salinity	Control	1.10 ± 0.18	1.16 ± 0.15
	Low	0.42 ± 0.68	−0.09 ± 0.16
	High	0.68 ± 0.20	0.31 ± 0.18
Nutrient depletion	Control	0.90 ± 0.15	0.37 ± 0.15
	Nitrogen	1.01 ± 0.07	0.25 ± 0.16
	Phosphorous	1.00 ± 0.09	0.29 ± 0.11
	Silicon	0.61 ± 0.06	0.21 ± 0.17

The effect of irradiance on cell growth evaluated through fluorescence seemed to confirm what we observed in the previous plots, since we noticed a decrease in cell growth in both stress conditions at 72 h in both species (Supplementary Table S3).

The effect of irradiance on RNA amount was highlighted with *P. calliantha* starting from 48 h when considering the high irradiance condition, and at 72 h when considering low irradiance (Figure 2A), both compared to control conditions. In *P. multistriata* we observed a different trend: the content of RNA expressed in pg per cell in the control condition was much lower than the stressed ones, with the highest value found under low irradiance stress at 24 h (Figure 2B). The correlation plot evaluated in terms of cellular RNA content showed, on average, a strong correlation between all the experimental conditions in *P. calliantha* (Figure 2C). On the contrary, we observed a negative correlation (anticorrelation)

in control and low irradiance conditions compared to high irradiance (0.066 and −0.024, respectively), highlighting opposite trends of responses in terms of cellular activity (RNA content) with respect to high irradiance stress (Figure 2D).

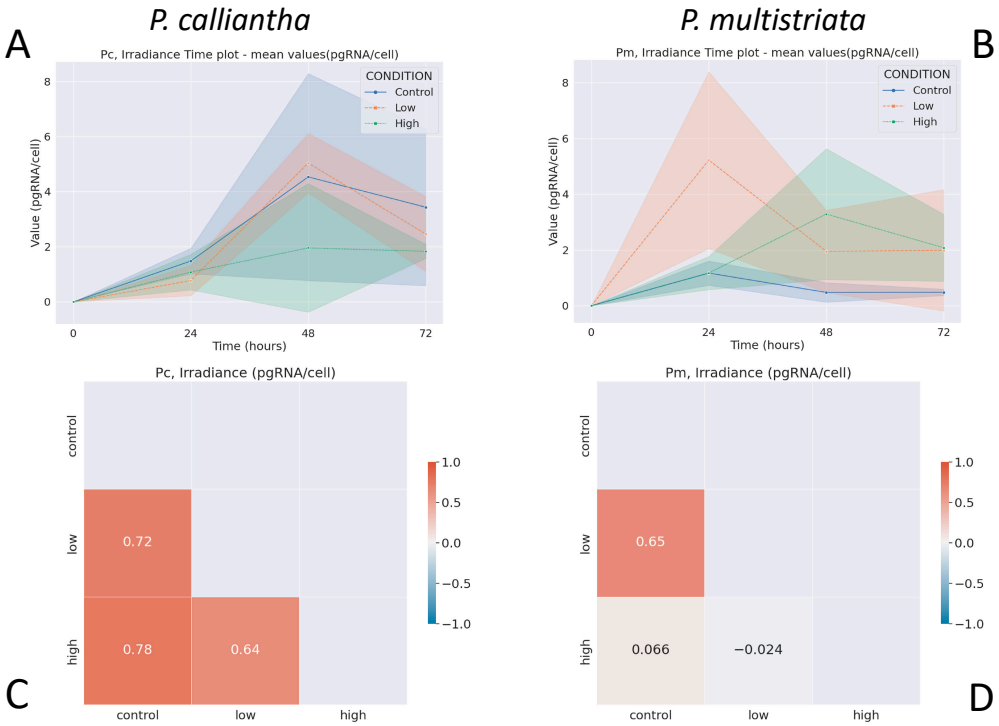

Figure 2. Time plots and correlation plots of pg RNA/cell mean values in response to irradiance in *P. calliantha* (**A**,**C**) and *P. multistriata* (**B**,**D**). An irradiance of 100, 45, and 350 µmol photons $m^{-2}s^{-1}$ was applied for the control, low, and high treatments, respectively. Standard deviations in time plots are shown as color bands, and can partially overlap.

By observing the regression line between cells/mL and fluorescence values in all the irradiance-stress experiments, we can confirm a marked positive correlation (ranging from 0.96 to 1) in all the considered conditions between the two variables used to evaluate cell growth (Supplementary Figure S1).

3.2. Temperature

The temperature for low and high treatments was 12 °C and 28 °C, respectively, compared to the control condition of 20 °C. Generally, high-temperature stress was not detrimental to cell growth in all clones, and algal density was comparable to that of control conditions. Temperature had a small effect on *P. calliantha* growth, except for a reduced growth when considering low temperature starting from 48 h (Figure 3A). In *P. multistriata*, we observed a marked specific growth rate decrease related to low temperature conditions compared to control and high-temperature conditions starting from 24 h (Figure 3B). The correlation plots in response to cell growth and temperature variations showed a widespread strong correlation between *P. calliantha* and *P. multistriata*, highlighting a similar behavior in all the experimental conditions in the corresponding time plots (Figure 3C,D). Two-way ANOVA tests performed on both cell-concentration experiments showed significant differences when considering condition*time datasets (p-value of 0.001 and 0.003 for *P. calliantha* and *P. multistriata*, respectively), and non-significant differences when considering condition datasets (Supplementary Tables S1 and S2).

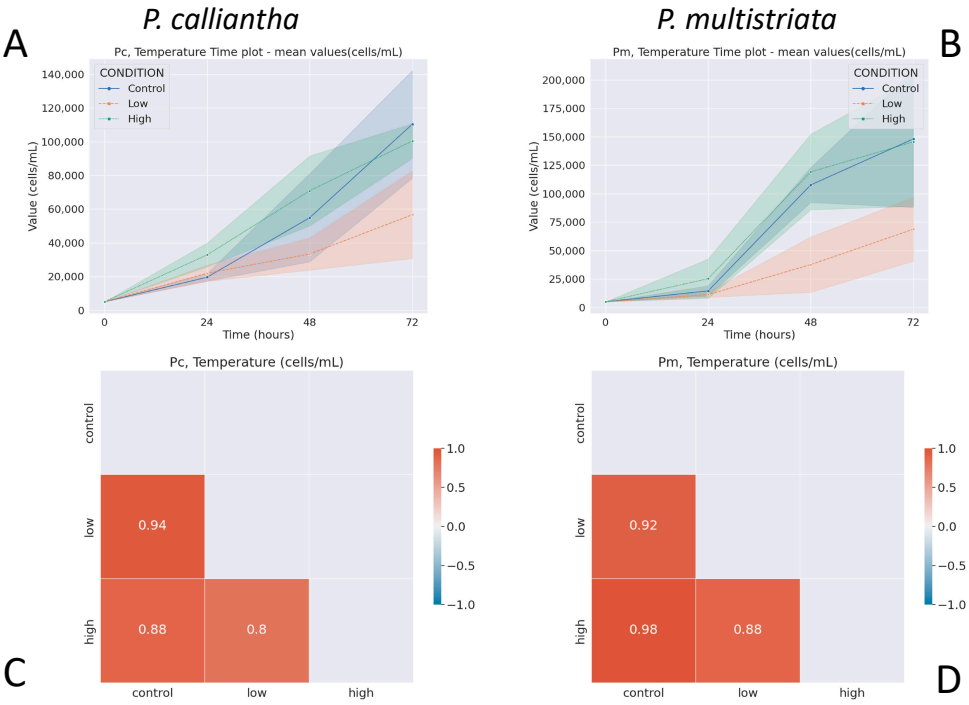

Figure 3. Time plots and correlation plots of cells/mL mean values in response to temperature in *P. calliantha* (**A**,**C**) and *P. multistriata* (**B**,**D**). Temperature for the control, low, and high treatments was 20, 12, and 28 °C, respectively. Standard deviations in time plots are shown as color bands, and can partially overlap.

The μ values (Table 2) confirmed a decrease in the low-temperature condition in both species, compared to control and high-temperature conditions.

The previous trends of cell growth were also confirmed by data from the fluorescence experiments, with a decrease in the cell density related to low- and high-temperature conditions when compared to the control condition (Supplementary Table S4).

The effect of temperature on RNA content per cell of *P. calliantha* was strongly manifested at high temperatures, with a general decrease in the mean values starting from 24 h (Figure 4A). In *P. multistriata* the low-temperature condition was the most divergent from the other experimental conditions, with a general increase in the RNA content per cell at 48 and 72 h (Figure 4B). The correlation plot of this parameter in *P. calliantha* showed a moderate correlation between all the considered experimental conditions (Figure 4C). In *P. multistriata*, however, there was a weak correlation between low and high temperature, with the opposite behavior of RNA content per cell when considering 24 and 48 h time points (Figure 4D).

Finally, by investigating the regression line between cells/mL and fluorescence values in all the temperature-stress experiments, we can confirm a clearly positive correlation (ranging from 0.96 to 1) between these two variables in all the tested conditions (Supplementary Figure S2).

3.3. Salinity

Salinity effect on *P. multistriata* and *P. calliantha* was evaluated by setting low and high salinity at 34 and 38 PSU, respectively, compared to the 36 PSU of the control condition. The effect of salinity on cell growth (considering both the cells/mL and fluorescence values) was distinguishable at 72 h in both species with a marked reduction in specific growth rate of *P. calliantha*, and zero growth of *P. multistriata*, for both high and low salinity, compared to the control condition (Figure 5A,B). The correlation plot highlighted, in *P. calliantha*, a widespread correlation among the specific growth rates for all experimental conditions, with a maximum of 0.92 in the low versus high salinity correlation (Figure 5C

and Supplementary Table S5). However, we observed an opposite trend in *P. multistriata*. In this case, there were no correlations among the three considered conditions, with a significant negative correlation (−0.67) between low and high salinity stresses (Figure 5D), highlighting a different response for each considered experiment. Two-way ANOVA tests performed on both cell-concentration experiments showed significant differences when considering condition*time datasets only for *P. calliantha* species (*p*-value of 0.04), and non-significant differences when considering condition datasets (Supplementary Tables S1 and S2).

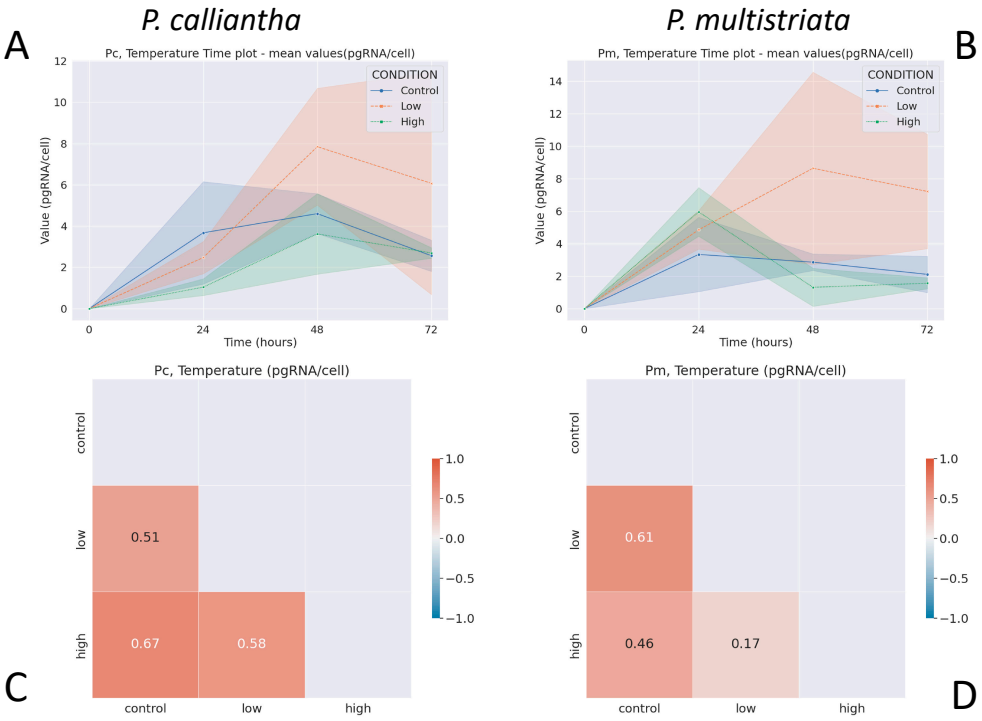

Figure 4. Time plots and correlation plots of pg RNA/cell mean values in response to temperature in *P. calliantha* (**A**,**C**) and *P. multistriata* (**B**,**D**). Temperature for the control, low, and high treatments was 20, 12, and 28 °C, respectively. Standard deviations in time plots are shown as color bands, and can partially overlap.

The specific growth rates of both species (Table 2) confirmed a marked decrease in low- and high-salinity-stress conditions, compared to the control condition. In particular, the growth rate in the low-salinity condition had a negative value.

Considering the content of RNA per cell in response to salinity, we observed higher RNA levels for the low-salinity condition in the time plots of *P. calliantha* and *P. multistriata* for all the considered times, and a marked response to the high-salinity condition at 24 h in the time plot of *P. multistriata*, when compared to the control condition (Figure 6A,B). The correlation plot of salinity responses, evaluated in terms of RNA content per cell, highlighted a moderate correlation between all the experiments in both *P. calliantha* and *P. multistriata* species (Figure 6C,D).

By analyzing the regression line between cells/mL and fluorescence values in all the salinity-stress experiments, we can confirm a clear positive correlation, with a Pearson correlation coefficient ranging from 0.81 to 0.98, between the two variables in all the considered conditions (Supplementary Figure S3). However, we noticed an exception for *P. multistriata* exposed to high salinity stress, where a moderate positive correlation (0.6) between the two variables was found (Supplementary Figure S3f).

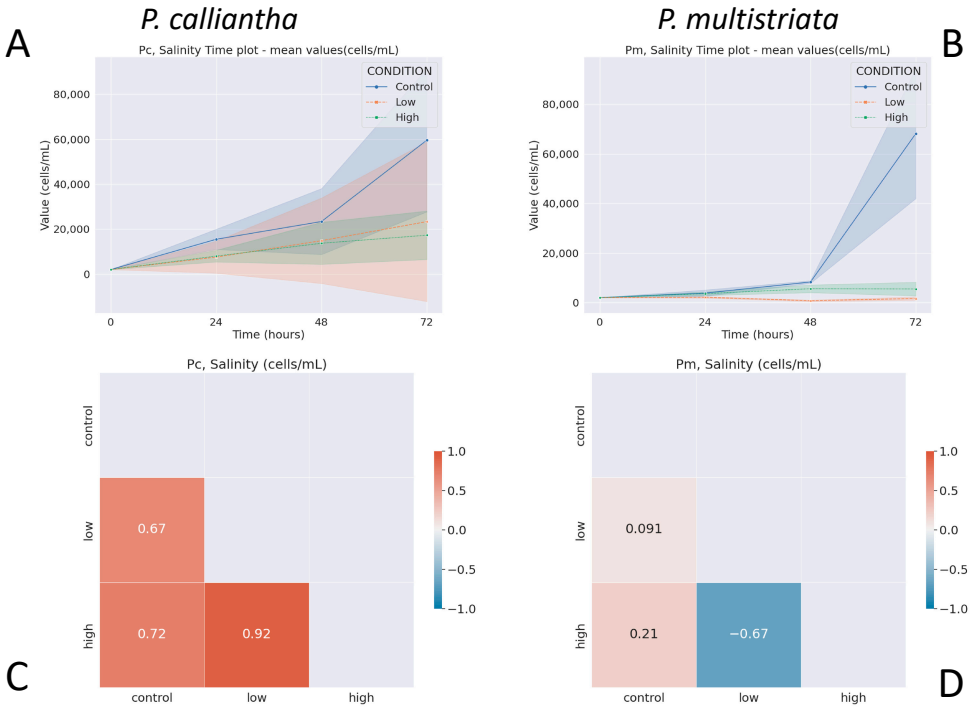

Figure 5. Time plots and correlation plots of cells/mL mean values in response to salinity in *P. calliantha* (**A**,**C**) and *P. multistriata* (**B**,**D**). Salinity effect was evaluated by setting control, low, and high salinity at 36, 34, and 38 PSU, respectively. Standard deviations in time plots are shown as color bands, and can partially overlap.

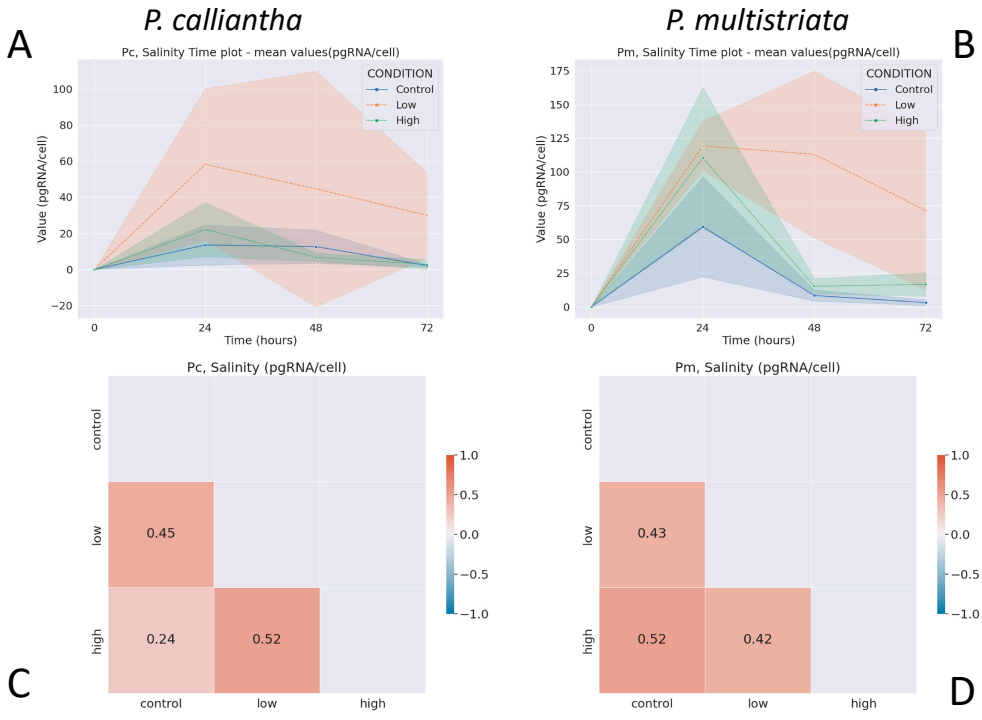

Figure 6. Time plots and correlation plots of pg RNA/cell mean values in response to salinity in *P. calliantha* (**A**,**C**) and *P. multistriata* (**B**,**D**). Salinity effect was evaluated by setting control, low, and high salinity at 36, 34, and 38 PSU, respectively. Standard deviations in time plots are shown as color bands, and can partially overlap.

3.4. Nutrient Depletion

Nutrient depletion was evaluated through the elimination of $NaNO_3$, $NaH_2PO_4 \cdot H_2O$, or $Na_2SiO_3 \cdot 9H_2O$ from the f/2 culture medium. The effect of nutrient depletion on cell growth, considering both cells/mL and fluorescence mean values, was appreciable in *P. calliantha* under silicon depletion, with a decrease in the specific growth rate starting from 48 h with respect to other experimental conditions (Figure 7A, Table 2). In *P. multistriata*, however, the effect of depletion was highlighted for all the investigated nutrients when considering the cells/mL mean values, with a general decrease in the respective specific growth rates when compared to control conditions (Figure 7B). Considering the results of the fluorescence experiments, we observed a decrease only in the silica curve, starting from 48 h (Figure 7). In any case, the correlation plots related to responses to the stresses in terms of cell growth highlighted, on average, strong correlation between all the performed experiments for both species, with similar trends in all the curves of time plots (Figure 7C,D, Supplementary Table S6). Two-way ANOVA tests performed on both cell-concentration experiments showed significant differences when considering condition*time datasets (*p*-value of 0.0006 and 0.0001 for *P. calliantha* and *P. multistriata*, respectively), and non-significant differences when considering condition datasets (Supplementary Tables S1 and S2).

Specific growth rate values related to nutrient depletion were very similar to each other, with the exception of the slight decrease in the silica-depletion experiments of both species (Table 2).

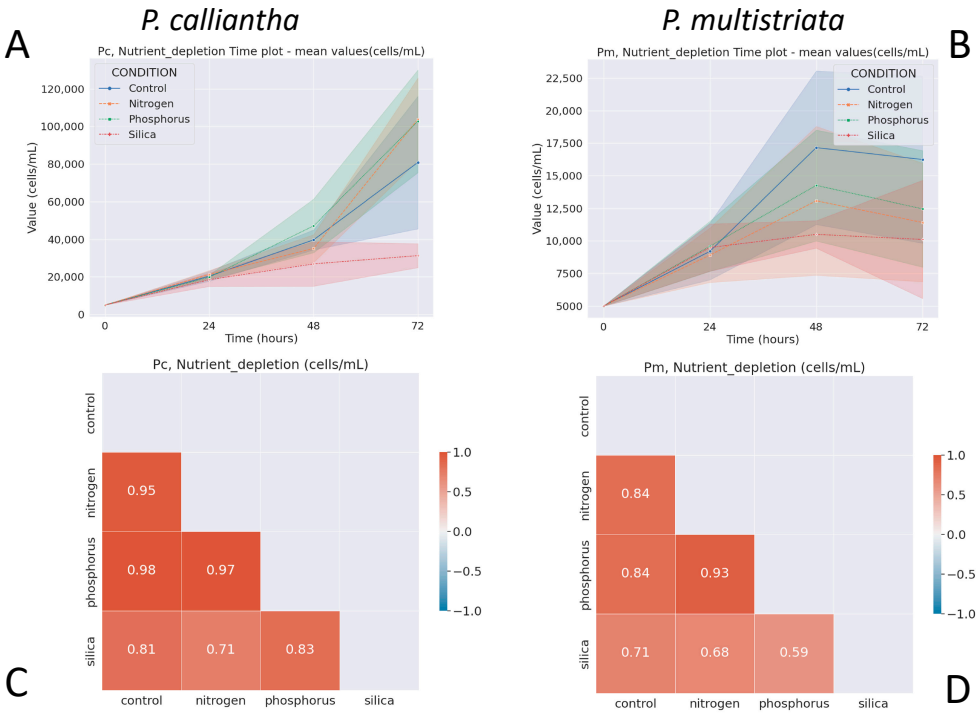

Figure 7. Time plots and correlation plots of cells/mL mean values in response to nutrient depletion in *P. calliantha* (**A**,**C**) and *P. multistriata* (**B**,**D**). Nutrient depletion was evaluated by using cells cultured in f/2 medium as control condition, and comparing it to those maintained in media deprived of $NaNO_3$, K_2HPO_4, or Na_2SiO_3. Standard deviations in time plots are shown as color bands, and can partially overlap.

Nutrient depletion affected the RNA content per cell in *P. calliantha* with an increase in the RNA levels between 24 and 48 h for the experiments involving silica in comparison to other conditions (Figure 8A). In *P. multistriata*, we observed higher levels of RNA per cell from 48 to 72 h for silica and nitrogen depletions when compared to control and phosphorous conditions (Figure 8B). The correlation plots for the nutrient-depletion

responses for RNA content per cell highlighted values ranging from moderate to strong correlations for both species, except for nitrogen- and silicon-depleted conditions in *P. calliantha* (0.19, Figure 8C,D).

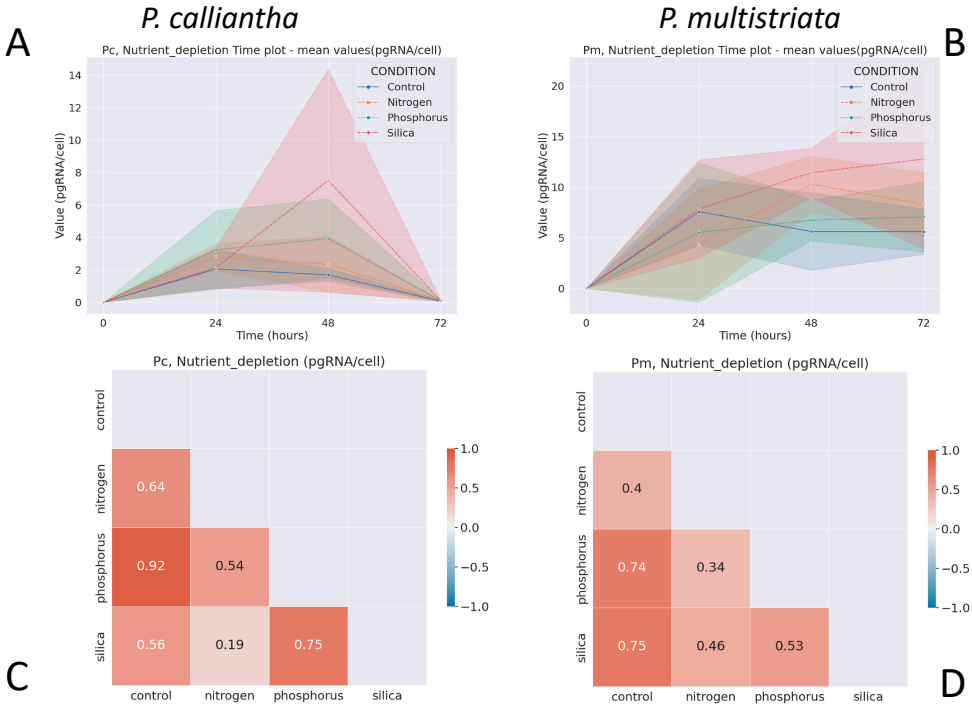

Figure 8. Time plots and correlation plots of pg RNA/cell mean values in response to nutrient depletion in *P. calliantha* (**A**,**C**) and *P. multistriata* (**B**,**D**). Nutrient depletion was evaluated by using cells cultured in f/2 medium as control condition, and comparing it to those maintained in media deprived of $NaNO_3$, K_2HPO_4, or Na_2SiO_3. Standard deviations in time plots are shown as color bands, and can partially overlap.

By observing the regression line between cells/mL and fluorescence values in all the nutrient-depletion experiments, we can confirm a marked positive correlation (ranging from 0.94 to 0.99) for *P. calliantha* in all the considered conditions between these two variables (Supplementary Figure S4A–D), and a moderate positive correlation (ranging from 0.22 to 0.47) in all the considered conditions in *P. multistriata* (Supplementary Figure S4E–H).

4. Discussion

In this paper, we analyzed the effect of physical and nutritional parameters on cell growth of six clones belonging to the species *P. calliantha* and *P. multistriata*. To summarize a general overview of all the responses of both species to each tested condition, evaluated in terms of cells/mL, we represented all stressful conditions in the heatmap below (Figure 9).

Generally, a high intraspecific variability in terms of cell density was observed for all clones in all tested conditions since individual strains can react differently to stressful conditions. This behaviour was also highlighted by the high standard deviations found for both Pm and Pc clones, suggesting that, for each species, different strains can have different levels of resilience to unfavourable culture conditions. This suggests that, within the same species, some clones can be more adaptable than others and thus more able to survive under specific abiotic stresses.

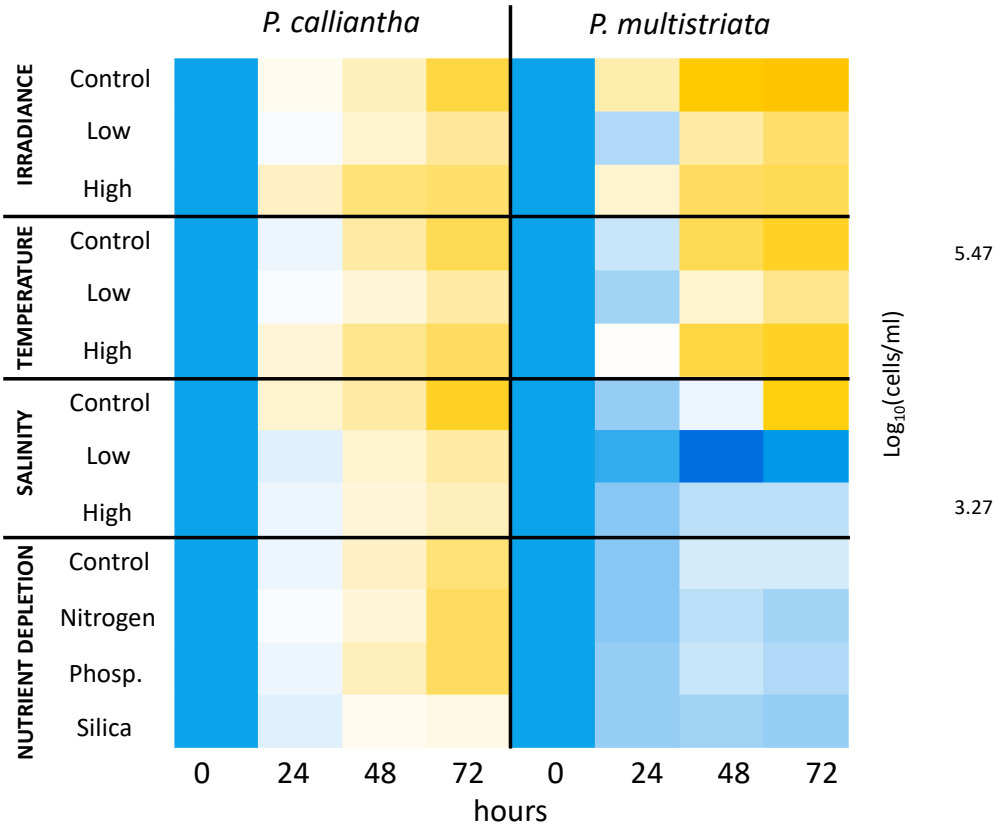

Figure 9. Overview of the responses of both species to all the considered stress conditions, evaluated in terms of Log_{10} (cells/mL) over time. Low levels of cells/mL are shown in blue, while high levels of cells/mL are shown in orange.

Considering the interspecific differences, the clones of *P. calliantha* showed higher specific growth rates (μ) than those of *P. multistriata* in both control (i.e., optimal) and stressful conditions. Moreover, *P. multistriata* species were more sensitive to temperature, irradiance, salinity, and nutrient stresses and showed a higher sensitivity and a faster response in terms of growth reduction with respect to control conditions. However, for all clones, no particular detrimental effects in terms of μ were observed at high temperatures. This suggests that occurrence of algal blooms of both species are still possible considering the actual climatic conditions, characterized by a gradual increase in water temperature, even if HABs are also influenced by other drivers, such as nutrient loads due to anthropogenic activities, which render it difficult to predict their occurrence and intensity [27]. A reduction in cell growth was also observed at high and low irradiances, and in this case the effect was more marked under low light, indicating the importance of light availability to cell growth. The more drastic reductions of algal growth were observed in cells exposed to low (34) or high (38) salinities, suggesting that slight variations in this parameter can dramatically impact their growth. This consideration was enforced by the significant negative correlation between these two conditions in *P. multistriata*. Regarding nutrients, silicon caused a more drastic slowdown in cell density, as observed in other diatoms [28]. Indeed, silicon is essential for frustule synthesis, so culturing algae in media amended with small amounts of this nutrient reduces cell division and, thus, their concentration [29]. Reduction in cell density under non-optimal conditions is a very common phenomenon that has already been observed in microalgae [28,30–32], while the true distinctive feature of our experiments was the general increase in RNA content under certain kinds of abiotic stress. However, in some cases this parameter did not show a precise trend, and varied over time and among different clones. A marked effect of the high-stress condition was confirmed by the negative correlation between high irradiance and the other two conditions, and by no

significant correlation between high and low temperature conditions. RNA increase was particularly evident in cultures exposed to low salinities, in Pm clones in hypersaline media, and under low-temperature stress and silicon depletion. This could be associated with the stenohaline nature of the test species [16]. The same low-temperature effect was observed in the model freshwater species Chlamydomonas reinhardtii by Hessen and co-workers, who hypothesized that RNA increase was due to a compensatory mechanism aimed at avoiding a reduction in protein synthesis [33]. Regarding nutrients, a slight increase in RNA amount per cell was observed under nitrogen and phosphorous depletion in Pm clones after 48–72 h of exposure, while silicon caused a more immediate increase. In Pc clones, a lower increase in RNA under nutrient depletion suggests that they had a better resilience against nutrient stress. In a previous work performed by using the diatom Thalassiosira weissflogii as test organism, a reduction in RNA content to one third was observed under nitrogen limitation [34]. The response of our species was different, since we performed experiments by completely depleting this nutrient, and this harsh condition could cause a slight increase in RNA content in Pc and Pm species to overcome nitrogen stress. On the basis of these few works, we can speculate that the Pseudo-nitzschia clones increase their RNA content per cell and this possibly reflects increased transcriptional activity probably stimulated by stress conditions; however, above certain thresholds of tolerance, these algae trigger a series of catabolic processes, including RNA degradation, which ultimately cause cell death. This hypothesis is in agreement with the mounting of a stress response and could also reflect other associated responses like retrotransposon activities [35]. However, our hypothesis should be corroborated by additional analyses, since RNA abundance is not, per se, sufficient to satisfactorily explain the molecular mechanisms involved in abiotic stress in algal cells. Firstly, experiments with longer time exposure, to assess the effect of stressful conditions on RNA over time, are mandatory to confirm our hypothesis. Assessment of the specific RNA families expressed and total RNAseq experiments on the Pseudo-nitzschia clones will support a deeper evaluation of the transcriptomic response of these algae under optimal and harsh conditions, promoting the investigation of activated or repressed pathways or genes involved in stress response and the understanding of the algal responses and reactions to counteract the effects of detrimental growth conditions. In parallel, quantification of the specific RNA content could be followed by tailored design of RNA microarrays to address the variability of the responses. In this way, we could expand these studies with efficient molecular tools to investigate specificities and similarities at different level of granularities among strains and species under harsh conditions.

5. Conclusions

In the present work, we exposed six clones belonging to two bloom-forming species (*P. calliantha* and *P. multistriata*) to different abiotic stresses, to assess culture conditions enhancing or inhibiting the proliferation of these toxic diatoms, widely distributed in temperate and warm waters and often responsible for harmful algal blooms. To monitor their growth and their resilience in unfavorable conditions, we used conventional methods (evaluation of specific growth rates) and a fast molecular assessment through the quantification of the total amount of RNA per cell, to identify features that could be associated with the stress response. Abiotic stresses caused a general reduction in the specific growth rates of all the tested strains, with a higher sensitivity of *P. multistriata* clones. Low temperatures, salinity fluctuations, and silicon depletion seemed to be the most detrimental conditions for these species. Moreover, we observed a general increase in RNA content of cells exposed to unfavorable culture conditions, which could have been due to an increase in cellular activity to counteract the effects of the applied stresses. Although additional efforts are needed to expand our analyses and clarify the cause of the RNA content variability, as well as its specific nature, we can hypothesize that RNA content in algal cells could be considered a key variable in implementing efficient molecular tools for fast detection of signs of stress in microalgae.

Supplementary Materials: The following supporting information can be downloaded at: https://www.mdpi.com/article/10.3390/jmse11091743/s1, Supplementary Table S1. Two-way ANOVA tests without replication related to *P. calliantha* cell-concentration experiments; Supplementary Table S2. Two-way ANOVA tests without replication related to *P. multistriata* cell-concentration experiments; Supplementary Table S3. Fluorescence values expressed as relative fluorescence intensity in arbitrary units (AU) related to the irradiance-stress experiments. Measurement times were 0, 24, 48, and 72 h (T0, T1, T2, and T3, respectively), for both *P. calliantha* and *P. multistriata* species (Pc and Pm, respectively). Standard deviations for each fluorescence value are also shown; Supplementary Table S4. Fluorescence values expressed as relative fluorescence intensity in arbitrary units (AU) related to the temperature-stress experiments. Measurement times were 0, 24, 48, and 72 h (T0, T1, T2, and T3, respectively) for both *P. calliantha* and *P. multistriata* species (Pc and Pm, respectively). Standard deviations for each fluorescence value are also shown; Supplementary Table S5. Fluorescence values expressed as relative fluorescence intensity in arbitrary units (AU) related to the salinity-stress experiments. Measurement times were 0, 24, 48, and 72 h (T0, T1, T2, and T3, respectively) for both *P. calliantha* and *P. multistriata* species (Pc and Pm, respectively). Standard deviations for each fluorescence value are also shown; Supplementary Table S6. Fluorescence values expressed as relative fluorescence intensity in arbitrary units (AU) related to the nutrient-depletion-stress experiments. Measurement times were 0, 24, 48, and 72 h (T0, T1, T2, and T3, respectively) for both *P. calliantha* and *P. multistriata* species (Pc and Pm, respectively). Standard deviations for each fluorescence value are also shown; Supplementary Figure S1. Scatter plots and related regression lines of cells/mL versus fluorescence values in irradiance-stress experiments in *P. calliantha* (A–C) and *P. multistriata* (D–F), in control (A,D), low (B,E), and high (C,F) irradiance-stress condition. An irradiance of 100, 45, and 350 µmol $m^{-2}s^{-1}$ was applied for the control, low, and high treatments, respectively; Supplementary Figure S2. Scatter plots and related regression lines of cells/mL versus fluorescence values in temperature-stress experiments in *P. calliantha* (A–C) and *P. multistriata* (D–F), in control (A,D), low (B,E), and high (C,F) temperature-stress condition. Temperature for the control, low, and high treatments was 20, 12, and 28 °C, respectively; Supplementary Figure S3. Scatter plots and related regression lines of cells/mL versus fluorescence values in salinity-stress experiments in *P. calliantha* (A–C) and *P. multistriata* (D–F), in control (A,D), low (B,E), and high (C,F) salinity-stress conditions. Salinity effect was evaluated by setting control, low, and high salinity at 36, 34, and 38 PSU, respectively; Supplementary Figure S4. Scatter plots and related regression lines of cells/mL versus fluorescence values in nutrient-depletion-stress experiments in *P. calliantha* (A–D) and *P. multistriata* (E–H), in control (A,E), nitrogen- (B,F), phosphorous- (C,G), and silica- (D,H) depletion conditions. Nutrient depletion was evaluated by using cells cultured in f/2 medium as control condition, and comparing it to those maintained in media deprived of $NaNO_3$, K_2HPO_4, or Na_2SiO_3.

Author Contributions: L.A., M.M., L.B. and A.S., study conception and design; L.B., data collection; L.A. and M.M., statistical analyses; L.A., M.M., L.B. and A.S., first draft of the manuscript; M.L.C., R.C. and M.F.: critical revision; S.G.: supervision. All authors have read and agreed to the published version of the manuscript.

Funding: This research received no external funding.

Institutional Review Board Statement: Not applicable.

Informed Consent Statement: Not applicable.

Acknowledgments: The authors are grateful to Eleonora Scalco (Research Infrastructures for Marine Biological Resources Department—Classic and Molecular Taxonomy Unit) for technical support. The scientific assistance of Wiebe Kooistra in assessing the experimental setup was greatly appreciated. The authors also wish to thank the editor and reviewers of the manuscript for their useful contributions in the improvement of the manuscript.

Conflicts of Interest: The authors declare no conflict of interest.

References

1. Kaparapu, J. Application of Microalgae in Aquaculture. *Phykos* **2008**, *48*, 21–26.
2. Fernández-Rodríguez, M.J.; Hidalgo-Lara, C.; Jiménez-Rodríguez, A.; Serrano, L. Bloom-Forming Microalgae in High-Species Phytoplankton Assemblages Under Light-Fluctuating and Low Phosphate Conditions. *Estuaries Coasts* **2015**, *38*, 1642–1655. [CrossRef]

3. Watson, S.B.; Whitton, B.A.; Higgins, S.N.; Paerl, H.W.; Brooks, B.W.; Wehr, J.D. Harmful Algal Blooms. In *Freshwater Algae of North America*; Wehr, J.D., Sheath, R.G., Kociolek, J.P., Eds.; Academic Press: Boston, MA, USA, 2015; pp. 873–920.
4. Masó, M.; Garcés, E. Harmful microalgae blooms (HAB); problematic and conditions that induce them. *Mar Pollut. Bull.* **2006**, *53*, 620–630. [CrossRef] [PubMed]
5. Pulido, O.M. Domoic acid toxicologic pathology: A review. *Mar. Drugs.* **2008**, *6*, 180–219. [CrossRef]
6. Bates, S.S.; Trainer, V.L. The Ecology of Harmful Diatoms. In *Ecology of Harmful Algae*; Granéli, E., Turner, J.T., Eds.; Springer: Berlin/Heidelberg, Germany, 2006; pp. 81–93.
7. Trainer, V.L.; Hickey, B.M.; Bates, S.S. (Eds.) *Toxic Diatoms*; Elsevier: New York, NY, USA, 2008; pp. 219–239.
8. Stocker, T.F.; Qin, D.; Plattner, G.K.; Alexander, L.V.; Allen, S.K.; Bindoff, N.L.; Bréon, F.M.; Church, J.A.; Cubasch, U.; Emori, S.; et al. Technical Summary. In *Climate Change 2013—The Physical Science Basis: Working Group I Contribution to the Fifth Assessment Report of the Intergovernmental Panel on Climate Change*; Intergovernmental Panel on Climate, Ed.; Cambridge University Press: Cambridge, UK, 2014; pp. 31–116.
9. Dashkova, V.; Malashenkov, D.V.; Baishulakova, A.; Davidson, T.A.; Vorobjev, I.A.; Jeppesen, E.; Barteneva, N.S. Changes in Phytoplankton Community Composition and Phytoplankton Cell Size in Response to Nitrogen Availability Depend on Temperature. *Microorganisms* **2022**, *10*, 1322. [CrossRef] [PubMed]
10. Anderson, D.M.; Glibert, P.M.; Burkholder, J.M. Harmful algal blooms and eutrophication: Nutrient sources, composition, and consequences. *Estuaries* **2002**, *25*, 704–726. [CrossRef]
11. Glibert, P.M.; Allen, J.I.; Bouwman, A.F.; Brown, C.W.; Flynn, K.J.; Lewitus, A.J.; Madden, C.J. Modeling of HABs and eutrophication: Status, advances, challenges. *J. Mar. Syst.* **2010**, *83*, 262–275. [CrossRef]
12. Glibert, P.M.; Seitzinger, S.; Heil, C.A.; Burkholder, J.M.; Parrow, M.W.; Codispoti, L.A.; Kelly, V. The role of eutrophication in the global proliferation of harmful algal blooms new perspectives and new approaches. *Oceanography* **2005**, *18*, 198–209. [CrossRef]
13. McCoy, G.R.; Touzet, N.; Fleming, G.T.; Raine, R. An evaluation of the applicability of microarrays for monitoring toxic algae in Irish coastal waters. *Environ. Sci. Pollut. Res.* **2013**, *20*, 6751–6764. [CrossRef]
14. Trainer, V.L.; Bates, S.S.; Lundholm, N.; Thessen, A.E.; Cochlan, W.P.; Adams, N.G.; Trick, C.G. *Pseudo-nitzschia* physiological ecology, phylogeny, toxicity, monitoring and impacts on ecosystem health. *Harmful Algae* **2012**, *14*, 271–300. [CrossRef]
15. Lewis, J.; Medlin, L.; Raine, R. MIDTAL (Microarrays for the Detection of Toxic Algae): A Protocol for a Successful Microarray Hybridisation and Analysis. *Phytotaxa* **2013**, *127*, 201–210.
16. McCoy, G.R.; Kegel, J.U.; Touzet, N.; Fleming, G.T.A.; Medlin, L.K.; Raine, R. An assessment of RNA content in *Prymnesium parvum*, *Prymnesium polylepis*, cf. *Chattonella* sp. and *Karlodinium veneficum* under varying environmental conditions for calibrating an RNA microarray for species detection. *FEMS Microbiol. Ecol.* **2014**, *88*, 140–159. [CrossRef]
17. Kegel, J.U.; Del Amo, Y.; Medlin, L.K. Introduction to project MIDTAL: Its methods and samples from Arcachon Bay, France. *Environ. Sci. Pollut. Res.* **2013**, *20*, 6690–6704. [CrossRef] [PubMed]
18. Barra, L.; Ruggiero, M.V.; Sarno, D.; Montresor, M.; Kooistra, W. Strengths and weaknesses of microarray approaches to detect *Pseudo-nitzschia* species in the field. *Environ. Sci. Pollut. Res.* **2013**, *20*, 6705–6718. [CrossRef] [PubMed]
19. Dittami, S.M.; Edvardsen, B. Culture conditions influence cellular rna content in ichthyotoxic flagellates of the genus *Pseudochattonella* (dictyochophyceae) 1. *J. Phycol.* **2012**, *48*, 1050–1055. [CrossRef] [PubMed]
20. Kegel, J.U.; Del Amo, Y.; Costes, L.; Medlin, L.K. Testing a microarray to detect and monitor toxic microalgae in Arcachon Bay in France. *Microarrays* **2013**, *2*, 1–23. [CrossRef] [PubMed]
21. Guillard, R.R. Culture of phytoplankton for feeding marine invertebrates. In *Culture of Marine Invertebrate Animals*; Smith, W.L., Chanley, M.H., Eds.; Springer: Boston, MA, USA, 1975; pp. 29–60.
22. Van Rossum, G.; Drake, F. *Python 3 Reference Manual*; CreateSpace: Scotts Valley, CA, USA, 2009.
23. Harris, C.R.; Millman, K.J.; Van Der Walt, S.J.; Gommers, R.; Virtanen, P.; Cournapeau, D.; Wieser, E.; Taylor, J.; Berg, S.; Smith, N. Array programming with NumPy. *Nature* **2020**, *585*, 357–362. [CrossRef]
24. McKinney, W. Data structures for statistical computing in python. In Proceedings of the 9th Python in Science Conference, Austin, TX, USA, 28 June–3 July 2010; pp. 51–56.
25. Waskom, M.L. Seaborn: Statistical Data Visualization. *J. Open Source Softw.* **2021**, *6*, 3021. [CrossRef]
26. Babicki, S.; Arndt, D.; Marcu, A.; Liang, Y.; Grant, J.R.; Maciejewski, A.; Wishart, D.S. Heatmapper: Web-enabled heat mapping for all. *Nucleic Acids Res.* **2016**, *44*, W147–W153. [CrossRef]
27. Gobler, C.J. Climate Change and Harmful Algal Blooms: Insights and perspective. *Harmful Algae* **2020**, *91*, 101731. [CrossRef]
28. d'Ippolito, G.; Sardo, A.; Paris, D.; Vella, F.M.; Adelfi, M.G.; Botte, P.; Gallo, C.; Fontana, A. Potential of lipid metabolism in marine diatoms for biofuel production. *Biotechnol. Biofuels* **2015**, *8*, 28. [CrossRef] [PubMed]
29. Martin-Jézéquel, V.; Hildebrand, M.; Brzezinski, M.A. Silicon metabolism in diatoms: Implications for growth. *J. Phycol.* **2000**, *36*, 821–840. [CrossRef]
30. Botte, P.; d'Ippolito, G.; Gallo, C.; Sardo, A.; Fontana, A. Combined exploitation of CO_2 and nutrient replenishment for increasing biomass and lipid productivity of the marine diatoms *Thalassiosira weissflogii* and *Cyclotella cryptica*. *J. Appl. Phycol.* **2018**, *30*, 243–251. [CrossRef]
31. Levitan, O.; Dinamarca, J.; Zelzion, E.; Lun, D.S.; Guerra, L.T.; Kim, M.K.; Kim, J.; Van Mooy, B.A.; Bhattacharya, D.; Falkowski, P.G. Remodeling of intermediate metabolism in the diatom *Phaeodactylum tricornutum* under nitrogen stress. *Proc. Natl. Acad. Sci. USA* **2015**, *112*, 412–417. [CrossRef]

32. Wiśniewska, K.; Śliwińska-Wilczewska, S.; Lewandowska, A.; Konik, M. The effect of abiotic factors on abundance and photosynthetic performance of airborne cyanobacteria and microalgae isolated from the southern Baltic Sea region. *Cells* **2021**, *10*, 103. [CrossRef] [PubMed]
33. Hessen, D.O.; Hafslund, O.T.; Andersen, T.; Broch, C.; Shala, N.K.; Wojewodzic, M.W. Changes in stoichiometry, cellular RNA, and alkaline phosphatase activity of *Chlamydomonas* in response to temperature and nutrients. *Front. Microbiol.* **2017**, *8*, 18. [CrossRef] [PubMed]
34. Olson, R.J.; Vaulot, D.; Chisholm, S.W. Effects of environmental stresses on the cell cycle of two marine phytoplankton species. *Plant Physiol.* **1986**, *80*, 918–925. [CrossRef]
35. Maumus, F.; Allen, A.E.; Mhiri, C.; Hu, H.H.; Jabbari, K.; Vardi, A.; Grandbastien, M.A.; Bowler, C. Potential impact of stress activated retrotransposons on genome evolution in a marine diatom. *BMC Genom.* **2009**, *10*, 624. [CrossRef]

Disclaimer/Publisher's Note: The statements, opinions and data contained in all publications are solely those of the individual author(s) and contributor(s) and not of MDPI and/or the editor(s). MDPI and/or the editor(s) disclaim responsibility for any injury to people or property resulting from any ideas, methods, instructions or products referred to in the content.